Ion-exchanged zeolite P as a nanostructured catalyst for biodiesel production

A. Al-Ani, Natalie E. Mordvinova, Oleg I Lebedev, Andrei Khodakov, V. Zholobenko

Energy Reports 5 (2019) 357–363

Contents lists available at ScienceDirect

Energy Reports

journal homepage: www.elsevier.com/locate/egyr

Research paper

Ion-exchanged zeolite P as a nanostructured catalyst for biodiesel production

Aqeel Al-Ani [a,b,*], Natalie E. Mordvinova [c], Oleg I. Lebedev [c], Andrei Y. Khodakov [d], Vladimir Zholobenko [a,*]

[a] Keele University, School of Physical and Chemical Sciences, Keele, ST5 5BG, UK
[b] Oil Marketing Company (SOMO), Baghdad, Iraq,
[c] Laboratoire CRISMAT ENSICAEN UMR CNRS 6508, 6 Boulevard du Maréchal Juin, 14050, Caen Cedex 04, France
[d] University Lille, CNRS, Centrale Lille, ENSCL, University Artois, UMR 8181 - UCCS - Unité de Catalyse et Chimie du Solide, F-59000 Lille, France

HIGHLIGHTS

- The potential of nano-sized zeolite MAP as a biorefinery catalyst is examined.
- The zeolite catalysts are characterised by TEM, NMR, XPS and XRD.
- Methanolysis of bio-oils is carried out using microwave heating.
- K-MAP shows the best catalytic performance in the conversion of bio-oils.
- High activity of K-MAP is due to its Al and K content and nanoparticle nature.

GRAPHICAL ABSTRACT

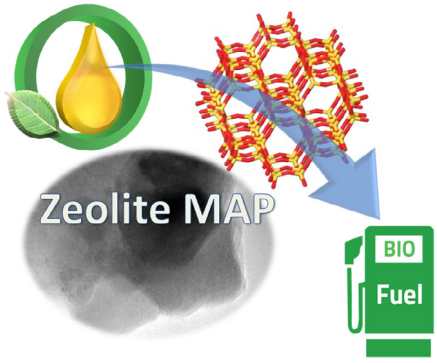

ARTICLE INFO

Article history:
Received 19 December 2018
Received in revised form 25 February 2019
Accepted 5 March 2019
Available online 13 March 2019

Keywords:
Synthetic gismondine
Zeolites
Transesterification
Basic sites
Nanostructured catalysts

ABSTRACT

Nano-crystalline synthetic gismondine modified via cation exchange has been utilised as a highly active and selective catalyst for the production of biofuel. In comparison with low silica zeolites FAU and LTA, K-form of gismondine, based on the maximum aluminium P (MAP) zeolite, exhibited a significant improvement in catalytic performance in the methanolysis of bio-oil, which can be attributed to its nano-particle morphology and high basicity associated with the high Al content and high degree of ion exchange, as demonstrated by the TEM, XRD, TGA, NMR, XPS and CO_2-TPD studies. To the best of our knowledge, this is the first report on a successful catalytic application of basic K-MAP zeolite.

1. Introduction

The production of biofuel as a sustainable energy source can be carried out in an environmentally friendly way by utilising heterogeneous, rather than homogeneous, catalysis involving zeolites, which would offer potential advantages, such as the elimination of the quenching step and associated aqueous waste, separation of the products, and the possibility to utilise a continuous reaction stream (Alzate et al., 2017; Esposito et al., 2017;

* Corresponding authors at: Keele University, School of Physical and Chemical Sciences, Keele, ST5 5BG, UK.
E-mail addresses: a.a.t.al-ani@keele.ac.uk (A. Al-Ani), v.l.zholobenko@keele.ac.uk (V. Zholobenko).

https://doi.org/10.1016/j.egyr.2019.03.003

Tan et al., 2017; Vaccaro, 2017; Ivars et al., 2018; Kordouli et al., 2018). Solid acid catalysts can be used to carry out the transformation of both triglycerides (TGs) and free fatty acids (FFA) simultaneously, however, such a process would require a longer reaction time and higher temperature, whereas solid basic catalysts achieve higher reaction rates in the transesterification of TGs or operate at lower temperatures (Goodwin et al., 2005; Serrano et al., 2018). Zeolitic materials have been widely exploited in many large-scale industrial processes (AbdulAziz et al., 2016; Daud et al., 2016a; Paixão et al., 2017; Perego et al., 2017; Doyle et al., 2018; Su et al., 2019), whereas their applications as solid bases are much less common (Yu et al., 2015; Dhepe and Chaudhary, 2017). Our recent work demonstrated that for the transesterification of TGs over hierarchical faujasites possessing intracrystalline networks of mesopores, the zeolite composition, and hence, the strength of basic sites has a greater effect on the activity of the catalyst than the accessibility of the porous structure of mesostructured zeolites (Al-Ani et al., 2018). The basic character of zeolites increases with rising aluminium content and higher concentration of more electropositive cations in the order Cs > K > Na > Li. Therefore, it can be expected that K- and Cs-forms of materials with lower Si/Al ratios, e.g. zeolites A (LTA structure type, Si/Al = 1), MAP (maximum aluminium P, GIS structure, Si/Al = 1), X and Y (FAU structure, Si/Al∼1.2 and 2.6, respectively) would be effective catalysts for some of the bio-refinery applications, such as transesterification and aldol condensation, which require a basic catalyst.

The purpose of the present work is to prepare, characterise and evaluate basic zeolites as catalysts in the production of biofuel. An essential part of this work is the detailed structural characterisation of basic zeolites in order to examine the role of the strength of basic sites and the accessibility of the pore network in the transformations of TGs.

This work is focused on the application of ion-exchanged zeolites with high aluminium content, such as gismondine, A, X and Y, as basic solid catalysts. The latter three materials are produced on a large scale and are widely used in ion-exchange, catalysis and separation. Gismondine, in the form of zeolite MAP with Si/Al ratio of 1.0, has also received a good deal of attention in the past owing to the unique flexibility of its crystalline framework (Fig. 1) and ion-exchange properties (Vezzalini et al., 1993; Araya, 1994; Adams et al., 1995, 1997; Zholobenko et al., 1998; Rohani et al., 2016; Sharma et al., 2016). This material was utilised in high performance detergents under the commercial name Doucil A24 in 1994. The chemical composition of A and MAP zeolites is almost identical, but there are significant differences in crystal structure and morphology, particle size, pore architecture and ion-exchange capacity. The superior ion-exchange properties and nano-size of its crystals, as reported by Adams et al. (1995), have been exploited in this work for the preparation of a basic cation-rich zeolite for the production of biofuels using TGs as a model biomass-derived feedstock. To the best of our knowledge, this is the first report on a successful catalytic application of zeolite MAP.

2. Materials and methodology

2.1. Materials

The parent NaY (CBV-100) and NaX (13X) zeolites were provided by Zeolysts International and Sigma-Aldrich. Zeolites NaA and NaMAP were obtained from Crosfield. Potassium nitrate (99.9%) and potassium hydroxide (86%) were supplied by Fisher Scientific. Refined rapeseed oil, caesium nitrate (99%), caesium hydroxide (99%) and methyl heptadecanoate (analytical GC standard, > 99.99%) were purchased from Sigma-Aldrich.

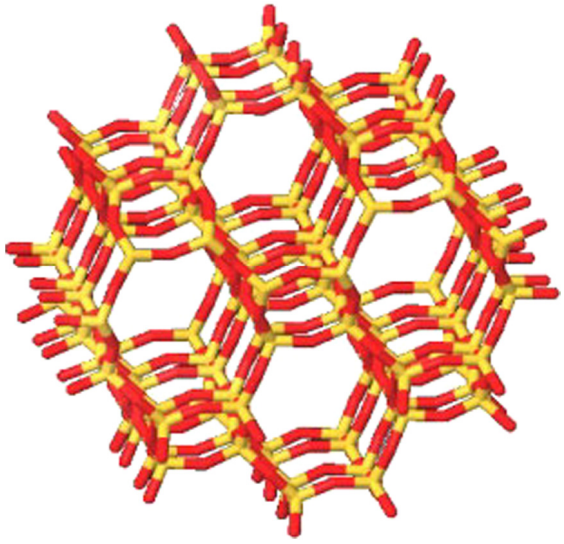

Fig. 1. NaMAP zeolite framework.

2.2. Preparation of the catalysts

The Cs-containing zeolites were prepared by treating the Na-forms of zeolites A, MAP , X and Y with 0.5 M of solution containing $CsNO_3$ and CsOH (4/1 v/v) at 80 °C for 1 h. To produce K-containing zeolites, ion exchange was carried out with 0.5 M solution containing KNO_3 and KOH (10/1 v/v) under the same conditions. The exchanged zeolites were washed with deionised water and dried at 80 °C overnight. The same protocol was utilised to obtain CsK-containing zeolites. These catalysts were produced by converting the Na-containing zeolites into their K-forms and then exchanging the latter with the Cs-containing solution. Before use, the zeolites were activated in a flow of air by heating from room temperature to the desired temperatures, up to 450 °C, at a rate of 1 °C/min and holding at the final temperature for 2 h.

2.3. Catalyst characterisation

Detailed structural characterisation of all the materials utilised in catalytic reactions was carried out using powder X-ray diffraction (XRD), scanning and transmission electron microscopy (SEM and TEM), thermogravimetric analysis (TGA), temperature-programmed desorption of carbon dioxide (CO_2-TPD), X-ray photoelectron spectroscopy (XPS), solid state nuclear magnetic resonance (^{27}Al MAS NMR) and nitrogen adsorption–desorption measurements. A comprehensive description of catalyst characterisation is presented in Electronic Supplementary Data (ESD) and in the literature (Al-Ani et al., 2018).

2.4. Reaction and reusability studies

The catalytic studies were conducted using a Biotage Initiator+ single-mode microwave system allowing to achieve high power density inside the batch reactors, which were specially designed 10- and 20-ml glass sealed vials utilised at high temperature and pressure (up to 160 °C and 15 bar). Typically, 10 ml of rapeseed oil was reacted in a 20-ml glass vial with methanol at a 1:6, 1:9 or 1:12 molar ratio at the range of temperatures between 100–160 °C for up to 1 h with continuous stirring utilising 1–5 wt% of the zeolite (relative to the mass of oil). In addition, some experiments were repeated using a conventionally

heated high-pressure reaction system, Monowave-50 supplied by Anton Paar, under continuous stirring in 10-ml glass vials as reactors at the same temperature and pressure as for microwave experiments (temperature ramp of ~40 °C/min). At the end of the reaction, the liquid products were separated and analysed using gas chromatography and the % conversion (ester content) was determined. The selectivity towards fatty acid methyl esters (FAMEs) was calculated without taking into account the glycerol produced.

The ester content of fatty acid methyl esters in biofuel was also determined according to the standard test method EN-14103. The internal standard solution of methyl heptadecanoate was prepared with concentration of 10 mg/mL in n-heptane. 0.1 ml of the purified reaction products was dissolved in 2 ml of the internal standard solution and then injected in to the Agilent 6890 GC equipped with an FID and the same column that was used in the characterisation of oils (see Table S1, ESD). The peak area for the ester components of the FAME C14:0 to C24:1 was used to calculate their mass fraction in percent (see Equation below):

$$C = (\sum A - AEI)/AEI \times (CEI \times VEI/m) \times 100\%$$

Where C is the ester content in percent, $\sum A$ is the total peak area from C14:0 to C24:1, AEI is the peak area of internal standard solution, CEI is the concentration of internal standard solution in mg/ml, VEI is the volume of internal standard solution in ml and m is the mass of sample in mg.

The turnover frequencies were calculated from the conversion values corresponding to 15 min reaction time and the number of basic sites obtained from CO_2-TPD experiments described in ESD.

Following the transesterification reaction, the catalyst was separated, washed with methanol 3 times and dried overnight at 60 °C. The dried zeolite was calcined under the same conditions as prior to the initial reaction and utilised again in the transesterification of rapeseed oil. The same reaction conditions were used in the consecutive runs for the recycled catalyst.

3. Results and discussion

Structural characterisation of Na-forms of the parent zeolites, which are standard commercially available samples, reveals typical features of these materials including small particle size and water loss upon heating (see Fig. 2 and Fig. S1, ESD).

TGA data for the hydrated NaMAP sample (Fig. 2) showed ~20 wt% loss of water between 25 and 350 °C, corresponding to 16 H_2O molecules per unit cell (u.c.). Both TGA and DTA indicated a three-stage water desorption, which has been assigned to the presence of different phases of zeolite MAP and different locations of H_2O molecules in the structure. ~4 wt% of water desorbed below 70 °C (3.5 mol/u.c.) is probably removed from mesopores rather than from the micropores indicating that the actual u.c. composition is $Na_8Al_8Si_8O_{32}$ ~13 H_2O in agreement with previous study (Zholobenko et al., 1998).

K-forms of these zeolites also demonstrate high thermal stability up to at least 450 °C and crystallinity (Fig. S2), although a significant line broadening is observed in the XRD patterns of zeolite MAP (Fig. 3 and Fig. S2, ESD), which is due to the small size of its crystalline domains (see below). For the KMAP zeolite, a noticeable decrease in intensity of the XRD patterns is observed following its calcination at elevated temperatures, particularly above 350 °C, which could be attributed to the significant structural changes taking place upon hydration–dehydration of this material around 300 °C, as reported previously (Vezzalini et al., 1993; Zholobenko et al., 1998). Hence, the activation temperature for zeolite MAP prior to the reaction studies has been limited to 320 °C. ^{27}Al MAS NMR spectra for Na-forms of the studied

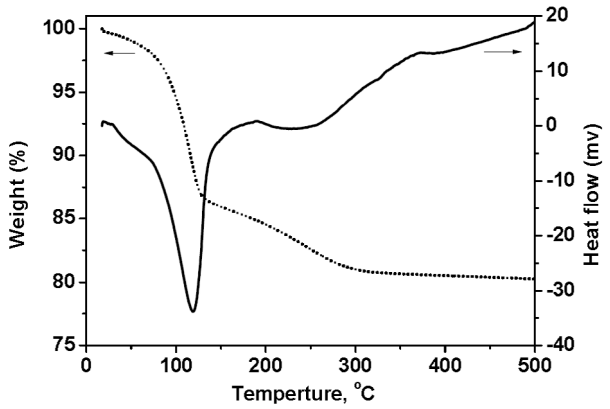

Fig. 2. TGA trace of the parent NaMAP zeolite.

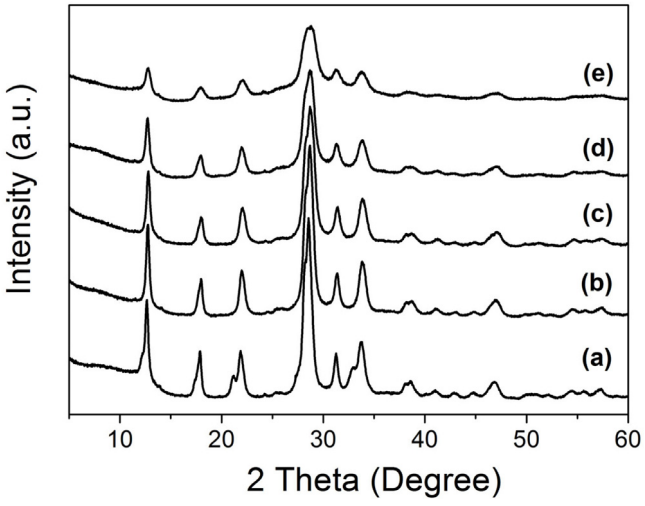

Fig. 3. Powder XRD patterns of KMAP zeolite activated at (a) 25 °C (b) 250 °C (c) 350 °C (d) 450 °C and (e) 550 °C.

zeolites (Fig. 4), show virtually no signal from extra-framework aluminium at ~0 ppm, which would have been indicative of the six-coordinate aluminium. The only intense Al signal detected at ~60 ppm is assigned to tetrahedrally coordinated species (Al_{tetr}), although the Al_{tetr} peak for NaMAP is asymmetrical, which is probably related to the aforementioned structural transitions in this zeolite caused by hydration–dehydration. The high ion-exchange capacity of the MAP zeolite, associated with the maximum Al content, allows the incorporation of a maximum amount of electropositive cations, such as K and Cs, thereby increasing the basicity of the framework oxygen (Al-Ani et al., 2018; Busca, 2017). In contrast, the degree of ion-exchange in zeolites A, X and Y is limited as some Na cations are located in small cages, including D6R and D4R units. This is supported by the chemical composition data for the studied ion-exchanged zeolites presented in Table S2.

The reaction studies (Fig. S3) carried out in a microwave batch reactor using K-containing zeolites MAP and A have shown a considerably higher activity as compared to the typical literature values (Barthomeuf, 1984; Blasco and Sánchez-Sánchez, 2009; Gedanken et al., 2016). Indeed, for KMAP, conversion over 90% at relatively low methanol to oil ratios is achieved after 15 min of reaction time with only 5 wt% of the catalyst at 160 °C (Fig. 5 and Fig. S4), whereas, conversion over 90% with ~100% selectivity towards fatty acid methyl esters (FAMEs) has been reported for

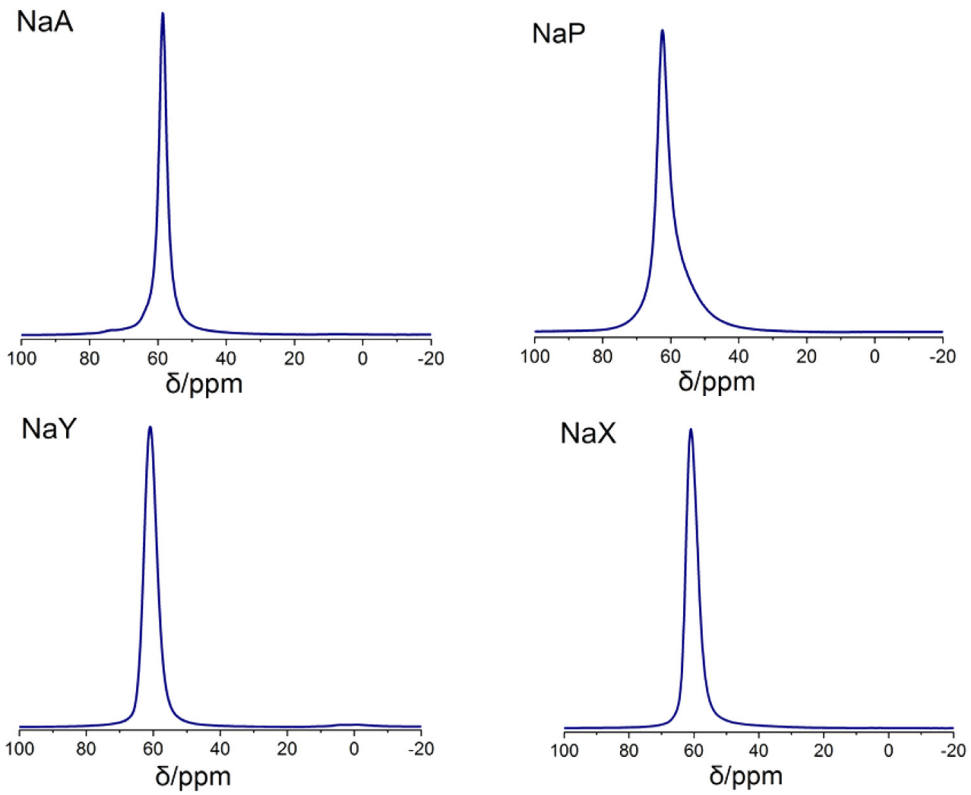

Fig. 4. ^{27}Al NMR spectra of NaA, NaMAP, NaY and NaX zeolites.

K_2O/NaX after 7 h of the reaction time (Romero et al., 2016). Overall, zeolite KMAP shows a higher activity in transesterification than KA, KX and KY type also demonstrating good recyclability and resistance to deactivation for three consecutive runs (Table 1 and Fig. 6). These findings are in good qualitative agreement with the chemical analysis data presented in Table S1. Indeed, zeolites A and MAP have the highest Al content (Si/Al = 1) and the degree of ion-exchange of sodium for potassium cations is the highest for zeolite MAP with K/Al ratio of ∼0.90. It should be noted that following the introduction of Cs cations into the Na-forms, the activity of faujasite type catalysts decreases, which can be explained by the lower degree of ion-exchange due to greater size of the Cs cations and almost no increase in the activity of CsKMAP and CsKA zeolites is observed as compared to their potassium forms (see Table 1). It could be expected that Cs-containing zeolites would be the strongest basic catalysts with the best performance in the transesterification reaction. However, in general, K-forms of the studied zeolites either matched the activity of their Cs-containing counterparts, or exceeded it (in the case of faujasites). This can be explained by a rather low degree of Cs-exchange, partial degradation of the zeolite structure or pore blockage due to the relatively severe conditions required for the introduction of Cs and by the formation of stable caesium carbonate species.

Although utilising microwave irradiation can lead to a faster and more efficient heating of the reaction mixture, possibly minimising the "wall effects" and suppressing the formation of by-products, our complementary studies using conventional heating mode in the Monowave 50 system have shown the conversion levels only ∼2% lower for the K-forms of zeolites A, MAP and X, which are within the experimental error margin. In addition, no unusual changes in the products distribution that could be attributed to the so-called microwave effects have been observed. The only significant difference discerned was the time required to reach the reaction temperature of 160 °C, this was ∼1 min for the microwave reactor and ∼4 min for the conventionally heated system.

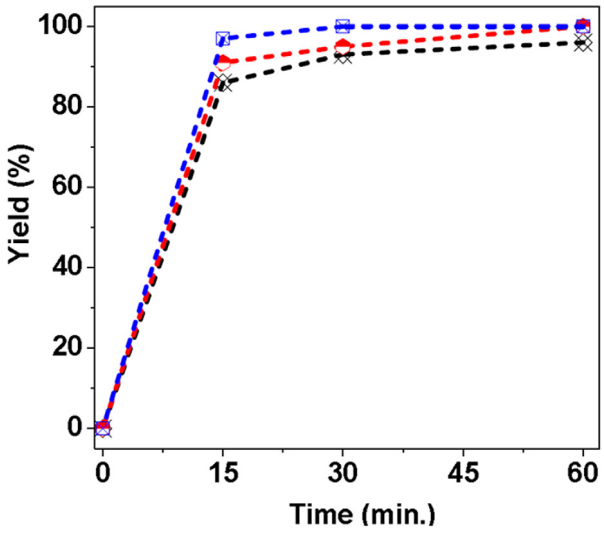

Fig. 5. The effect of the oil to methanol molar ratio: (--) black for 1:6; (--) red for 1:9 and (--) blue for 1:12. (For interpretation of the references to colour in this figure legend, the reader is referred to the web version of this article.)

The characterisation of basic sites in zeolites can be performed using a number of approaches, such as adsorption of probe molecules monitored by FTIR spectroscopy, XPS measurements and temperature programmed desorption of carbon dioxide (CO_2-TPD). FTIR spectra of test-molecules adsorbed on the cationic forms of zeolites have been reported in the literature (Barthomeuf, 1984; Blasco and Sánchez-Sánchez, 2009), however, to the best of our knowledge this approach has not been applied

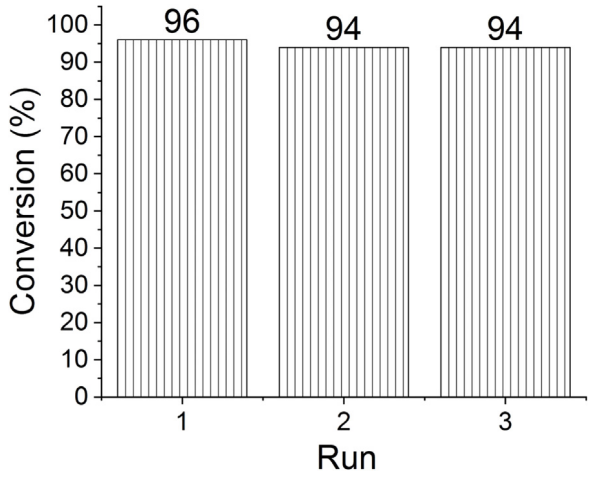

Fig. 6. The performance of the KMAP zeolite catalyst in the reusability experiment.

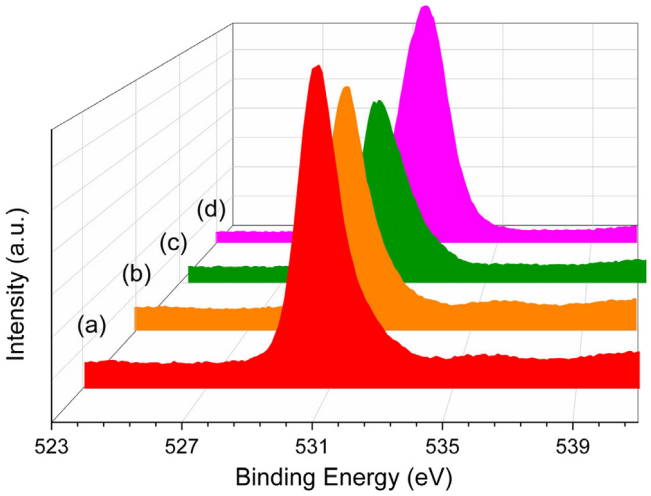

Fig. 8. Oxygen 1s XPS spectra of KMAP (a), KA (b), KX (c) and KY (d) zeolites.

to small-pore zeolites, such as MAP, and in general, only qualitative comparison of zeolites with similar structures, e.g. faujasites, has been successfully undertaken. Hence, the characterisation of the zeolite basic sites in this work has been based on the CO_2-TPD (Heidler et al., 1996; Hunger and Klepel, 2005; Wattanakit et al., 2017) and XPS analyses (Gruenert et al., 1994). The CO_2-TPD data summarised in Fig. 7 and Table S3 indicate that zeolite KMAP has the strongest basic sites (the highest T_{max} value of 290 °C); this can be explained by the greater negative charge on framework oxygen in KMAP owing to the high concentrations of K and Al (Si/Al = 1 and K/Al = 0.9). The total number of basic sites, which is approximately the same for KMAP, KA and KX (∼400 μmolg^{-1}), corresponds to 4–15 CO_2 molecules per nm^2 of the external surface, indicating that a considerable fraction of CO_2 can access the micropores of zeolites A and MAP under the experimental conditions at 100 °C, hence reducing certainty in the determination of the number of active sites, since the zeolite micropores are unlikely to be accessible to TG molecules. Indeed, our recent work demonstrates that the introduction of intracrystalline mesopores (∼4 nm) in faujasites does not lead to an improvement in their catalytic performance in the transesterification of TGs, which is largely dependent on the strength of basic sites, as methanolysis of TGs would require stronger basic sites as the pK_a of methanol is ∼15.5. However, the access to the porous structure of the hierarchical zeolites is important in other

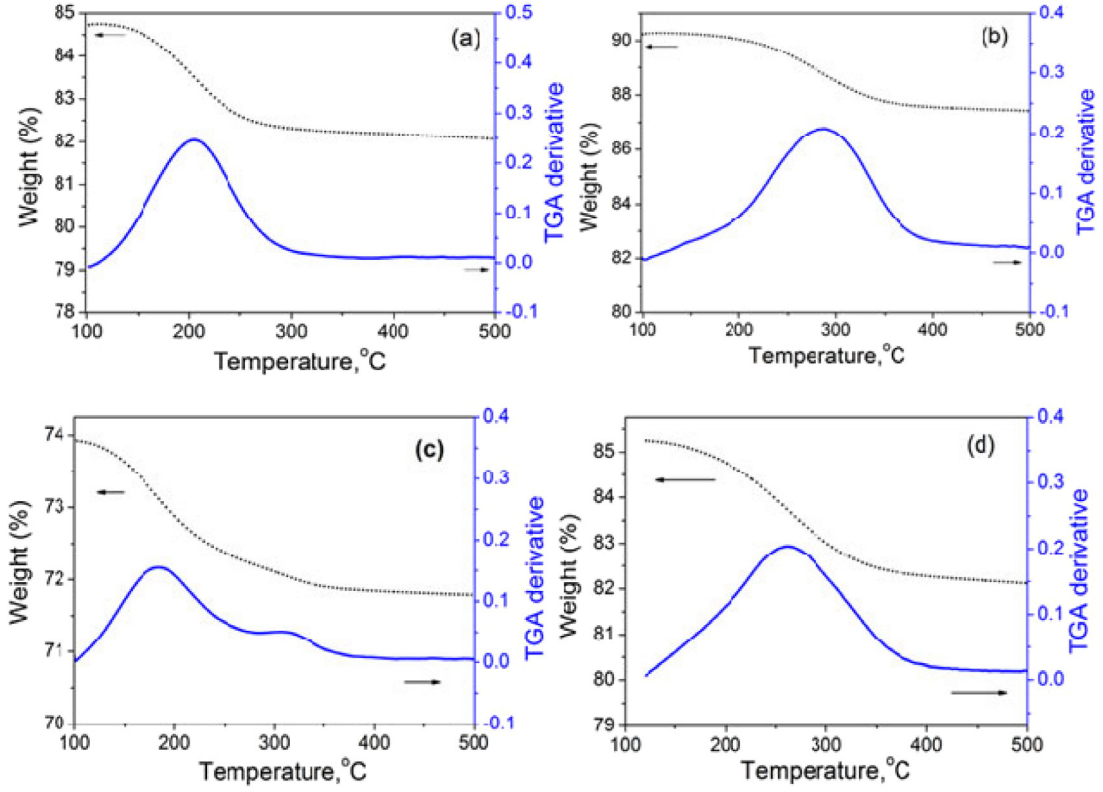

Fig. 7. CO_2-TPD profiles for (a) KA, (b) KMAP, (c) KY and (d) KX.

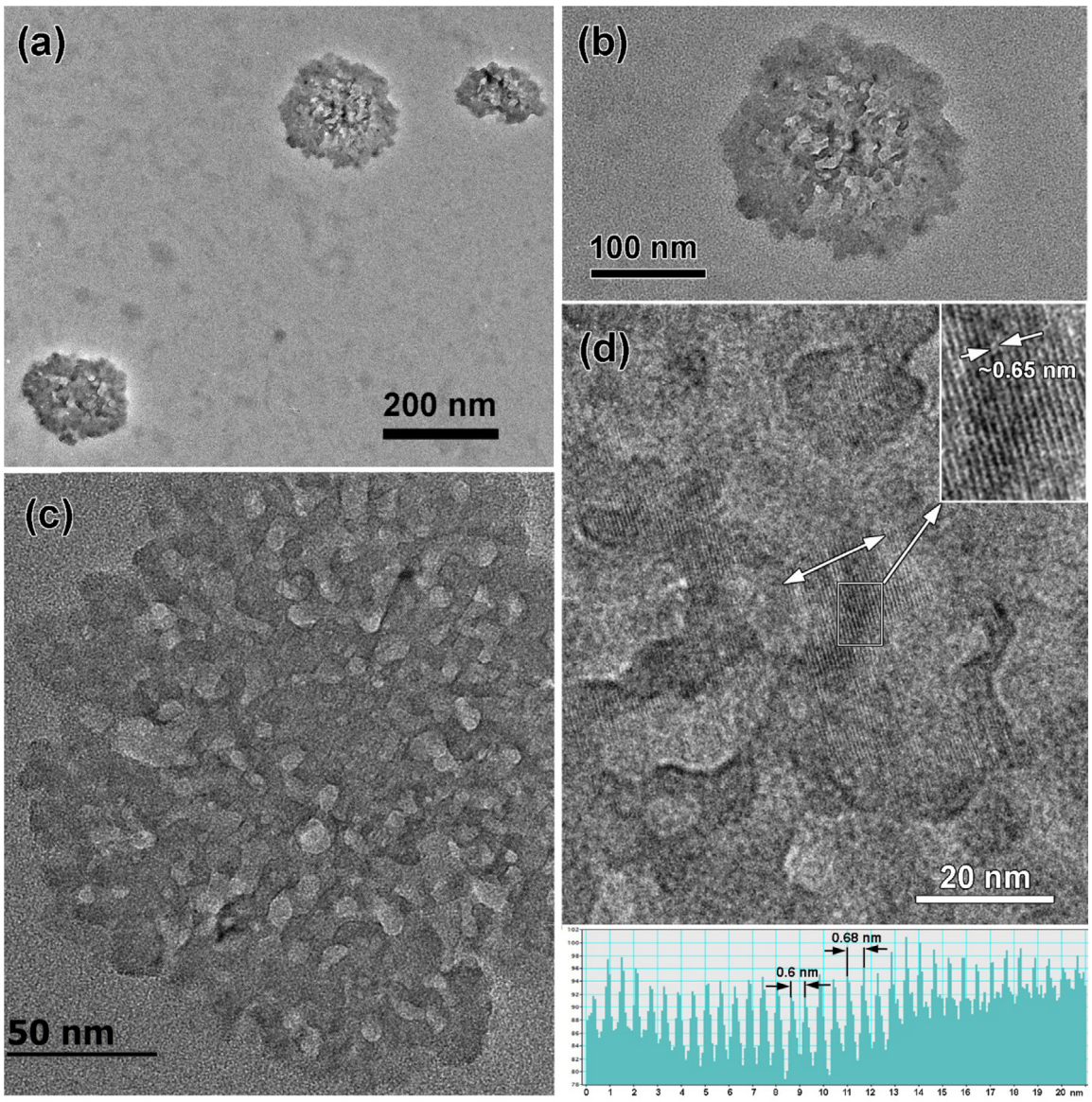

Fig. 9. TEM images of zeolite MAP showing its nano-sized crystallites at increasing magnification (a–c); (d) a high resolution section of the image highlighting the d-spacings in the zeolite.

zeolite for biodiesel production and bio-based platform chemicals (Daud et al., 2016b; Alaba et al., 2017; Wattanakit et al., 2017).

The strength of the basic sites on the external surface, which should determine the catalyst activity in the transesterification reaction, has been also assessed using XPS. As the basicity of the framework oxygen increases, reflecting its ability to donate an electron pair, the binding energy (BE) of the O_{1s} electrons would decrease (Gruenert et al., 1994). Indeed, as the data in Fig. 8 show, the O_{1s} BE decreases from 531.9 eV for KY (which demonstrates the lowest activity in the methanolysis of TGs) to 530.6 eV for KMAP and KA (which demonstrate the highest activity). The differences in the O_{1s} BE for the studied zeolites appear to be largely determined by their Si/Al ratio, which is the highest for zeolite Y (Si/Al = 2.5) and the lowest for zeolites A and MAP (Si/Al = 1). It should be noted that the zeolite activity in the transesterification reaction would also be affected by the accessibility of the active sites on the external surface, which would be greater for the MAP samples (see Table S2).

An important insight into the catalytic behaviour of zeolite MAP comes from the high resolution TEM imaging (Fig. 9). In accord with the published work (Adams et al., 1995), TEM data demonstrate the nano-scale features of this material with the size of the crystallites being ∼20 nm. This is in excellent agreement with the size of crystalline domains (18–20 nm) obtained from the XRD data using Scherrer equation; indeed, a significant line broadening for NaMAP can be seen in Fig. 3a (the TEM image of NaY zeolite is also presented in Fig. S.7 for comparison). Importantly, the crystallite size of MAP is ∼5–10 times smaller than that for zeolites X and Y (Table S4) resulting in a relatively high value for the external surface area of zeolite MAP, which may explain its high catalytic activity despite the fact that its micropores are inaccessible for the reacting molecules.

4. Conclusions

In summary, the application of zeolite based catalysts in the synthesis of biofuel can offer a greener production route potentially eliminating the need for corrosive chemicals and additional purification steps, and reducing the amount of aqueous waste. Nano-crystalline zeolite MAP and high aluminium content zeolites A, X and Y ion-exchanged with K and Cs have been utilised as highly active and selective catalysts in the transesterification

Table 1
Methanolysis of rapeseed oil with CH_3OH over basic zeolite catalysts.[a]

Zeolite	TOF (h^{-1})[b]	Conversion (%)	Selectivity (%)
NaMAP	12	3	>99
KMAP	202	96	>99
CsKMAP	–	98	>99
KA	140	65	>99
CsKA	–	67	>99
NaX	11	7	>99
KX	23	10	>99
CsNaX	–	5	>99
NaY	8	4	>99
KY	24	9	>99
CsNaY	–	4	>99

[a]Reaction conditions: reaction temperature 160°C, 5 wt% of catalyst based on the amount of oil; 1:12 oil to methanol molar ratio; reactions were carried out in triplicate, estimated error ±5 h^{-1}. For the analysis of the reaction products see Figs. S5 and S6.

[b]The turnover frequencies (TOF) were calculated from the conversion values corresponding to 15 minutes reaction time and the number of basic sites obtained from CO_2-TPD experiments.

of triglycerides demonstrating high activity and selectivity. The modified zeolites have been characterised by X-ray diffraction, scanning and transmission electron microscopy, TGA, CO_2-TPD and XPS. The data suggest that the enhanced catalytic performance of the K-form of zeolite MAP can be assigned to its high basicity, resulting from the high Al content and unique ion-exchange properties as well as nano-particle morphology with a relatively high external surface area available to the reacting species. This work highlights the potential of nano-sized zeolites for catalytic applications.

Acknowledgements

This work was supported by Oil Marketing Company (SOMO), Baghdad, Iraq under grant SL-144-03. The authors are grateful for the support of the Lennard-Jones Laboratories at Keele University, UK, where this study was carried out. The authors thank Riogen Company for providing reference samples of the faujasite type zeolites.

Appendix A. Supplementary data

Supplementary data, ESD, associated with this article can be found in the online version at https://doi.org/10.1016/j.egyr.2019.03.003.

References

AbdulAziz, A.R., Sani, Y.M., Alaba, P.A., Raji-Yahya, A.O., Daud, W.M.A.W., 2016. Facile synthesis of sulfated mesoporous Zr/ZSM-5 with improved Brønsted acidity and superior activity over SZr/Ag, SZr/Ti, and SZr/W in transforming UFO into biodiesel. J. Taiwan Inst. Chem. Eng. 60, 247–257.

Adams, C.J., Araya, A., Carr, S.W., Chapple, A.P., Franklin, K.R., Graham, P., et al., 1997. Zeolite MAP: the new detergent zeolite. In: Studies in Surface Science and Catalysis. Elsevier, pp. 1667–1674.

Adams, C.J., Araya, A., Carr, S.W., Chapple, A.P., Graham, P., Minihan, A.R., et al., 1995. Zeolite map: a new detergent builder. In: Studies in Surface Science and Catalysis. Elsevier, pp. 206–207.

Al-Ani, A., Zholobenko, V., Darton, R.J., Sneddon, S., 2018. Nanostructured zeolites: The introduction of intracrystalline mesoporosity in basic faujasite-type catalysts. ACS Appl. Nano Mater. 1, 310–318.

Alaba, P.A., Daud, W.M.A.W., Sani, Y.M., Mohammed, I.Y., Abakr, Y.A., 2017. Synthesis and characterization of sulfated hierarchical nanoporous faujasite zeolite for efficient transesterification of shea butter. J. Cleaner Prod. 142 (4), 1987–1993.

Alzate, C.A.C., Gutierrez, C.D.B., Serna, D.L.R., 2017. A comprehensive review on the implementation of the biorefinery concept in biodiesel production plants. Biofuel Res. J. 4 (3), 691–703.

Araya, A., 1994. US Pat., 5 362 466.

Barthomeuf, D., 1984. Conjugate acid–base pairs in zeolites. J. Phys. Chem. 88, 42–45.

Blasco, T., Sánchez-Sánchez, M., 2009. Characterization of zeolite basicity using probe molecules by means of infrared and solid-state NMR spectroscopies. Catal. Today 143, 293–301.

Busca, G., 2017. Acidity and basicity of zeolites: A fundamental approach. Microporous Mesoporous Mater. 254, 3–16.

Daud, W.M.A.W., AbdulAziz, A.R., Sani, Y.M., Alaba, P.A., Raji-Yahya, A.O., Mohammed, I.Y., Abakr, Y.A., 2016a. Synthesis and application of hierarchical mesoporous HZSM-5 for biodiesel production from shea butter. J. Taiwan Inst. Chem. Eng. 59, 405–412.

Daud, W.M.A.W., Alaba, P.A., Sani, Y.M., 2016b. Efficient biodiesel production via solid superacid catalysis: a critical review on recent breakthrough. RSC Adv. 6, 78351–78368.

Dhepe, P.L., Chaudhary, R., 2017. Solid base-catalyzed depolymerization of lignin into low molecular weight products. Green Chem. 3 (19), 778–788.

Doyle, A.M., Alismaeel, Z.T., Abbas, A.S., Albayati, T.M., 2018. Biodiesel from batch and continuous oleic acid esterification using zeolite catalysts. Fuel 234, 170–176.

Esposito, D., Brun, N., Hesemann, P., 2017. Expanding the biomass derived chemical space. Chem. Sci. 8 (7), 4724–4738.

Gedanken, A., Tangy, A., Pulidindi, I.N., 2016. SiO_2 beads decorated with SrO nanoparticles for biodiesel production from waste cooking oil using microwave irradiation. Energy Fuels 30, 3151–3160.

Goodwin, J.R., Lopez, D.E., Bruce, D.A., Lotero, E., 2005. Transesterification of triacetin with methanol on solid acid and base catalysts. Appl. Catal. A 295 (2), 97–105.

Gruenert, W., Muhler, M., Schroeder, K., Sauer, J., Schloegl, R., 1994. Investigations of zeolites by photoelectron and ion scattering spectroscopy. 2. A new interpretation of XPS binding energy shifts in zeolites. J. Phys. Chem. 98, 10920–10929.

Heidler, R., Janssens, G., Mortier, W., Schoonheydt, R., 1996. Charge sensitivity analysis of intrinsic basicity of faujasite-type zeolites using the electronegativity equalization method (EEM). J. Phys. Chem. 100, 19728–19734.

Hunger, B., Klepel, O., 2005. Temperature-programmed desorption (TPD) of carbon dioxide on alkali-metal cation-exchanged faujasite-type zeolites. J. Thermal Anal. Calorim. 80, 201–206.

Ivars, F., Zuliani, A., Luque, R., 2018. Advances in nanocatalyst design for biofuel production. ChemCatChem 10 (9), 1968–1981.

Kordouli, E., Pawelec, B., Bourikas, K., Kordulis, C., Fierro, J.L.G., Lycourghiotis, A., 2018. Mo promoted Ni-Al_2O_3 co-precipitated catalysts for green diesel production. Appl. Catal. B 229, 139–154.

Paixão, M.W., Jorge, E.Y., Lima, T.D.M., Lima, C.G., Marchini, L., Castelblanco, W.N., Rivera, D.G., Urquieta-González, E.A., Varma, R.S., 2017. Metal-exchanged magnetic β-zeolites: valorization of lignocellulosic biomass-derived compounds to platform chemicals. Green Chem. 19 (16), 3856–3868.

Perego, C., Bosetti, A., Ricci, M., Millini, R., 2017. Zeolite materials for biomass conversion to biofuel. Energy Fuels 31 (8), 7721–7733.

Rohani, S., Aldahri, T., Behin, J., Kazemian, H., 2016. Synthesis of zeolite Na-P from coal fly ash by thermo-sonochemical treatment. Fuel 182, 494–501.

Romero, R., Muciño, G.E.G., Garcia-Orozco, I., Serrano, A.R., Jiménez, R.B., Natividad, R., 2016. Deactivation study of K_2O/NaX and Na_2O/NaX catalysts for biodiesel production. Catal. Today 271, 220–226.

Serrano, D.P., Melero, J.A., Morales, G., Iglesia, S.J., Pizarro, P., 2018. Progress in the design of zeolite catalysts for biomass conversion into biofuels and bio-based chemicals. Catal. Rev. 60 (1), 1–70.

Sharma, P., Song, J., Han, M.H., Cho, C., 2016. GIS-NaP1 zeolite microspheres as potential water adsorption material: Influence of initial silica concentration on adsorptive and physical/topological properties. Sci. Rep. 6, 22734.

Su, M., Li, W., Zhang, T., Ma, Q., Fan, W., 2019. Production of liquid fuel intermediates from furfural via aldol condensation over potassium-promoted Sn-MFI catalyst. Fuel 237, 1281–1290.

Tan, T., He, M., Fang, Y., Baeyens, J., Wang, M., 2017. The Ni-Mo/γ-Al_2O_3 catalyzed hydrodeoxygenation of FAME to aviation fuel. Catal. Commun. 100, 237–241.

Vaccaro, L., 2017. Biofuels and green chemistry-a common journey ahead. Biofuel Res. J. 4 (4), 713–714.

Vezzalini, G., Quartieri, S., Alberti, A., 1993. Structural modifications induced by dehydration in the zeolite gismondine. Zeolites 13, 34–42.

Wattanakit, C., Yutthalekha, T., Suttipat, D., Salakhum, S., Thivasasith, A., Nokbin, S., Limtrakul, J., 2017. Aldol condensation of biomass-derived platform molecules over amine-grafted hierarchical FAU-type zeolite nanosheets (Zeolean) featuring basic sites. Chem. Commun. 53, 12185–12188.

Yu, J., Li, J., Corma, A., 2015. Synthesis of new zeolite structures. Chem. Soc. Rev. 44, 7112–7127.

Zholobenko, V., Chapple, A., Rhodes, N., Stuart, J., 1998. Structural transitions in zeolite P An in situ FTIR study. J. Chem. Soc. Faraday Trans. 94, 1779–1781.